

A millimeter-wave redshift survey of the bright S2-CLS population

S. C. Chapman^{1,2*},

¹*Department of Physics and Atmospheric Science, Dalhousie University, Halifax, NS, B3H 4R2, Canada*

²*NRC, Canada*

³*UBC, Canada*

⁴*MPI, Auf dem Hugel 71, D-53121 Bonn, Germany*

⁵*Centre for Extragalactic Astronomy, Department of Physics, Durham University, South Road, Durham DH1 3LE*

⁶*Centre for Astrophysics Research, Science & Technology Research Institute, University of Hertfordshire, Hatfield AL10 9AB, UK*

⁷*Harvard-Smithsonian Center for Astrophysics, 60 Garden Street, Cambridge, MA 02138*

⁸*Institute for Astronomy, University of Edinburgh, Royal Observatory, Blackford Hill, Edinburgh, EH9 3HJ, UK*

⁹*European Southern Observatory, Karl Schwarzschild Strasse 2, D-85748 Garching, Germany*

¹⁰*Department of Physics and Astronomy, UC Riverside, 900 University Avenue, Riverside, CA 92521*

Submitted for publication in MNRAS

ABSTRACT

We report on a blind, millimetre-wave redshift survey of the brightest, unlensed submillimetre galaxies (SMG) from the SCUBA-2, Cosmology Legacy Survey. From the Lockman Hole, AEGIS, and CDF-N fields, we selected the 14 brightest SMGs ($S_{850\mu\text{m}} > 11$ mJy) identified as single sources by the SMA. Using the IRAM NOEMA interferometer in two tunings with a combined 32 GHz bandwidth, we observed 12 of these 14 SMGs (two already had CO redshifts from previous observations), and detect at least one strong emission line in all galaxies. We assign precise spectroscopic redshifts to each of these 12 SMGs, unambiguously in four cases with two or more detected lines, and guided by photometric redshifts for the eight single line cases. The redshifts lie in the range $1.1 < z < 4.4$ with a median of 3.3. We highlight 2 (of 12) SMGs discovered blindly at $z > 4$ (lying at $z=4.14$ and $z=4.42$ respectively). Spectroscopic SMGs lying at these redshifts are still extremely rare, and it is remarkable that they were robustly discovered in this bright sample at a 17% success rate. We use the luminosities and widths of the CO lines, along with the SMA size constraints to infer the gas masses and dynamics of these HyLIRGs. While these SMGs are the most extreme galaxies known in the Universe, we do not typically find that they lie in strong redshift spikes identified through optical spectroscopic surveys.

Key words: galaxies: abundances – galaxies: high-redshift – submillimeter: galaxies.

1 INTRODUCTION

points to include

- up to 20mJy sources have turned up in relatively small area surveys at (sub)mm wavelengths (1700.850.1, 1549.850.8, GN20, other?) however. CLS shows that they are in fact very rare ...

- blind line surveys starting with Weiss of lensed source(s)

SMMJ, then Herschel lens surveys and SPT surveys,

- Chapman+15 first unlensed source blind z in CO.

- NOEMA capability

NEEDS: comparison with Bethermin model expectations?

brightest sources? SPT sources $N(z)$. GOODS-N filled in, and

L(COs) Q: AEGIS-1 lensed itzi? Lockman others? Field by

field comparison ... lock brights all $z=2.5$, $\text{GOODSN} < z >$

4! AEG. Help from Chris on interp?

-highlight $z > 4$ sources uniqueness

-highlight section on cdfn2 $z=4.4$... brightest source in this overdensity (17mJy) nothing else detected by SMA – overresolved by EXT config.

Blank-field mm and submm continuum surveys have discovered hundreds of dusty, star-forming submm galaxies (SMGs) over the past decade (e.g., Smail et al. 2002; Borys et al. 2003; Greve et al. 2004; Coppin et al. 2006; Bertoldi et al. 2007; Scott et al. 2008; Weiss et al. 2009), while *Herschel*-SPIRE has mapped close to 10^3 deg² in the 500, 350, 250 μm bands, leading to $\sim 10^4$ SMGs being detected (e.g., Oliver et al. 2010). At higher flux limits SPT has mapped 2500 deg² (e.g., Mocuano et al. 2013), and *Planck* has mapped the entire sky (Planck collaboration et al. 2014), finding many extreme and/or gravitationally lensed SMGs. The search for the most luminous star forming galaxies from 100's of deg² in the Universe has ensued (e.g., Fu et al. 2013, Ivison et al. 2013). However some of the SMGs discovered in early ~ 100 arcmin² surveys remain the intrinsically brightest, most extreme known (e.g., SMMJ02399 – Ivison et al. 1998, 2010, GN20 – Pope et al. 2006;

* scott.chapman@dal.ca

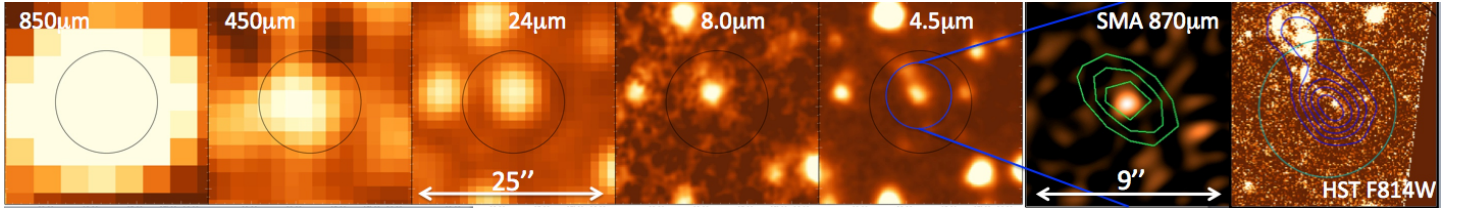


Figure 1. Example multi-wave cutout one of our sources, CDFN-1. From left to right: five cutout images $25''$ on a side of the longer wavelength data ($850\mu\text{m}$, $450\mu\text{m}$, $24\mu\text{m}$, $8\mu\text{m}$, $4.5\mu\text{m}$), highlighting the identification of the SMG with an IR-luminous component (black circle shows the $15''$ SCUBA-2 beam size). **Second from right:** A $9'' \times 9''$ zoom in from the SMA compact configuration $870\mu\text{m}$ map, with a $\sim 4''$ synthesized beam with PdBI $^{12}\text{CO}(4-3)$ contours overlaid. All of the SCUBA-2 flux (17 mJy) is recovered in a single compact component, unresolved with a $1.5''$ SMA beamsize. No other significant sources are detected within the $15''$ diameter of the SCUBA-2 beam. **Far right:** $9''$ cutout of the *HST*-ACS F814W image centred on the SMA detection, with IRAC ch-2 contours overlaid, shows CDFN-1 to be well identified with a faint tad-pole like $I_{AB} \sim 26$ galaxy, which is marginally detected in ground based imaging ($R = 26.1$).

Younger et al. 2008, and COSMOS-AzTEC1 – Scott et al. 2008; Younger et al. 2010).

Determining the redshifts of unlensed SMGs has largely been a process of using weak counterparts in the rest-frame ultraviolet and optical to make spectroscopic determinations (e.g., Chapman et al. 2003, 2005), or combining near- and mid-IR photometry to obtain reliable photometric redshift estimates (e.g., Wardlow et al. 2011; Simpson et al. 2014). However, because the high extinction of SMGs means that they often have only very faint (if any) counterparts in the optical/near-IR bands, the spectroscopic and even photometric redshift distributions have remained incomplete and biased (e.g., Simpson et al. 2014).

The largest spectroscopic SMG redshift survey to date was based on radio-identified SMGs (Chapman et al. 2005). The radio identification is sometimes inaccurate (Hodge et al. 2013) and may bias the redshift distribution since radio emission may remain undetected even in the deepest radio maps for sources at $z > 3$. Optical spectroscopic followup to ALMA-identified SMGs (Simpson et al. 2014; Danielson et al. 2018) have removed the identification bias, yet cannot remove the spectroscopic bias.

An alternative route to determine the redshift of an SMG is through observations of ^{12}CO emission lines at cm or mm wavelengths. The ^{12}CO lines arise from the molecular gas, the fuel for star formation, and can thus be related unambiguously to the submm continuum source. Therefore, these observations do not require any additional multi-wavelength identification and circumvent many of the problems inherent to optical spectroscopy of SMGs. However, to date the sensitivity of mm-wave facilities has limited the approach to followup of bright, gravitationally lensed SMGs (e.g., Weiss et al. 2009; Swinbank et al. 2010; Harris et al. 2012; Vieira et al. 2013; Zavala et al. 2015; Strandet et al. 2016).

While the IRAM Plateau de Bure Interferometer (PdBI) was sensitive enough to detect ^{12}CO in unlensed SMGs (e.g. Bothwell et al. 2013), its 3.6 GHz bandwidth receivers limit this approach due to the large time requirement for blind searches of ^{12}CO lines in redshift space via multiple frequency tunings. Walter et al. (2012) observed the HDF-N field with the PdBI over the full 3mm window to a similar depth as the Bothwell et al. (2013) survey, requiring 110 hrs on-source. In addition to blindly detecting two faint ^{12}CO emitting galaxies, they identified the redshift of the $S_{850\mu\text{m}} \sim 5\text{ mJy}$ HDF850.1 as $z = 5.3$. The 8-GHz instantaneous, dual-polarization bandwidth of ALMA, coupled with its sensitivity, improves this approach, but still makes it a relatively expensive prospect to blindly obtain ^{12}CO redshifts for even the brightest SMGs with $S_{850\mu\text{m}} \sim 8\text{ mJy}$.

In this paper, we describe a blind spectroscopic survey of

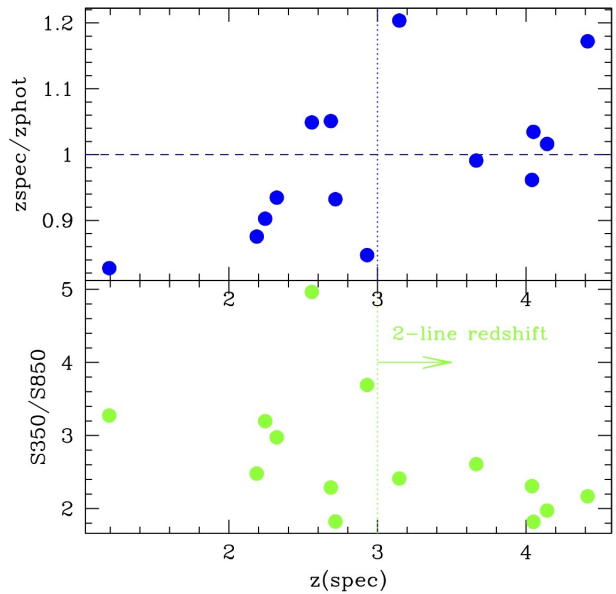


Figure 2. Top: Spectroscopic to photometric redshift as a function of spectroscopic redshift. Bottom: Flux ratio in 350 to 850 microns versus spectroscopic redshift. All sources with $z_{\text{spec}} > 3$ are identified with at least two robust $> 5\sigma$ emission line detections, and are considered secure. All sources with $z_{\text{spec}} < 3$ have only one detected emission line, and are placed at their most probably redshift based on SPIRE photometric analysis.

bright SMGs using the 16-GHz bandwidth of IRAM NOEMA with the Polyfix receiver, targeting primarily the ^{12}CO line emission in the 3mm band. The survey targets some of the brightest unlensed SMGs ever discovered in the northern CLS fields with $S_{850\mu\text{m}} > 11\text{ mJy}$ in a single SMA-identified source (Hill et al. 2018). The faintness of most of these SMGs at near-IR/optical wavelengths precluded optical spectroscopic observations (e.g., Hayward et al. 2018, despite lying in these well studied fields).

We use cosmological parameters $\Omega_m = 0.3$, $\Lambda = 0.7$, and $H = 70\text{ km s}^{-1}\text{ Mpc}^{-1}$ throughout the paper; at $z = 2.82$, this corresponds to an angular scale of $7.94\text{ kpc arcsec}^{-1}$, or $0.48\text{ Mpc arcmin}^{-1}$.

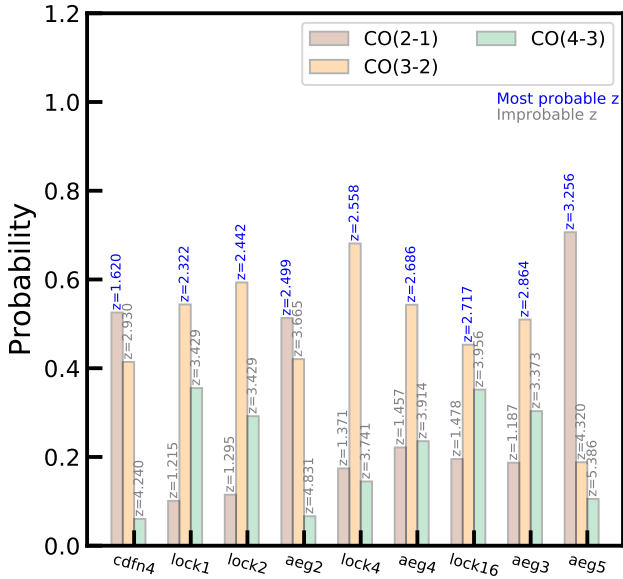


Figure 3. Quantized redshift possibilities and their probabilities for the 1-liners.

2 OBSERVATIONS AND STRATEGY

The sources were identified with SCUBA-2 at the JCMT as part of a submm-wave followup of 6 different extragalactic survey fields in the SCUBA-2 CLS. The brightest sources in the northern $850\mu\text{m}$ survey with $S_{850\mu\text{m}} > 11\text{mJy}$ in a single SMA-identified source were targeted for blind redshift followup with NOEMA Polyfix. Fig. 1 shows cutouts of an example source at SCUBA-2 and *Spitzer* wavelengths, with a clear identification at the various wavelengths.

IRAM-NOEMA observations targeting The Polyfix receiver’s 16 GHz wide spectrum revealed a strong line detected serendipitously at 150.6 GHz near the edge of the chosen 2mm-band setting (Figs. 2,3). Two followup observations targeted the three most likely redshifts, assuming this 150.6 GHz line was a ^{12}CO rotational transition, as described in § 3.1. We also draw on *Spitzer*-IRAC, ground-based and *HST* optical datasets described by Steidel et al. (2011). All flux measurements are shown in Fig. 4, and discussed in § 3.1.

2.1 IRAM/NOEMA Observations

The IRAM-NOEMA observations were taken in C or D configuration using the 10-12 antenna sub-arrays (properties of the observing runs and resulting synthesized beam sizes are summarized in Table 1), at a pointing centers defined by the SMA detections of each source at $850\mu\text{m}$. Flux calibration was achieved by observing various calibrators (3C273, 3C345, B0234+285, B1749+096). Phase and amplitude calibrators are also listed in Table 1. Data were processed using the most recent version of the GILDAS software. We resampled the cubes in 90 km s^{-1} channels, and imaged them using the GILDAS suite *mapping*, adopting natural weighting. The full NOEMA spectra is shown in Fig. 2-4. To obtain flux measurements, we deconvolved the visibilities using the CLEAN task with natural weighting, and applied the corresponding primary beam correction to the datacubes (which are negligible at the small $< 0.5''$ offset of the NOEMA position from the SMA position).

2.2 SMA observations

SMA observations were obtained for all sources as part of a followup campaign of the brightest 100 sources in the SCUBA-2 CLS survey, and are detailed in Hill et al. 2018. These observations in the compact configuration (beam sizes $\sim 2''$) in good weather ($\tau_{225\text{GHz}} \sim 0.08$) were obtained with the USB was tuned to 345 GHz, and combined with the LSB for an effective bandwidth of $\sim 4\text{ GHz}$ at 340 GHz, which yielded a final rms of $\sim 1\text{ mJy}$.

3 RESULTS

3.1 The redshift search

Our IRAM-NOEMA observations searched for the ^{12}CO and [CI] lines in these 12 SMGs. The source counts of the brightest submm sources ($S_{870\mu\text{m}} > 9\text{ mJy}$) measured by ALMA fall more steeply than those measured with lower resolution single-dish observations due to the multiplicity of the brightest sources when observed at arcsecond resolutions (e.g., Karim et al. 2013). However, these 12 sources were all resolved in a single component, typically retaining more than 90% of the S2 flux.

The IRAM-NOEMA observations showed double line detections in at the expected frequencies, and thereby implied that the proposed identification and redshift of $z \sim 2.31$ was incorrect. As the 7.2 GHz of frequency coverage did reveal a strong line detected serendipitously at 150.6 GHz near the edge of the 2mm setting, we began a search to identify the correct redshift. The centroid of this 150.6 GHz line detection, as well as the PdBI 2mm and 3mm continuum detections of SMA-CLS Nz, both localize the emission from the source within optical/IR imagery to within $\sim 0.5''$ (Fig. 1), while followup SMA $870\mu\text{m}$ continuum imaging unequivocally associates the $850\mu\text{m}$ SCUBA-2 source to a single IRAC galaxy which is well detected in the *HST* F814W image (Fig. 1) revealing a faint disturbed, tadpole-like galaxy. Ground-based imagery marginally detects the galaxy at $\mathcal{R} = 26.1$, $g = 27$, $U > 27.1$, making optical spectroscopy very difficult, and the $z = 2.82$ redshift would be difficult for near-IR spectroscopy, although the $K_{s,AB} = 23.2$ is feasible in general with a 10m telescope. Note that these colors (e.g., $g' - \mathcal{R} = 0.9\text{ mag}$) make sense for a heavily reddened object at $z=2.82$. However, the detection at g' -band, places loose constraints on the redshift to $z < 4$, while the comparable IRAC fluxes, $S(4.5\mu\text{m})=10.2\mu\text{Jy}$ and $S(8.0\mu\text{m})=13.2\mu\text{Jy}$ suggests the $1.6\mu\text{m}$ stellar bump should lie between, ranging between $2.4 < z < 3.7$. The very red $K_s - 4.5\mu\text{m}$ color (1.8 mags AB) is large, though consistent with a high stellar mass object. The MIPS $24\mu\text{m}$ flux of 0.17 mJy compared to the $S_{850\mu\text{m}}$ flux suggests that PAH emission is not contributing to the $24\mu\text{m}$ band, pushing the redshift to $z > 2.5$, as illustrated in the SED template fit (Fig. 4). Our final constraint on the redshift comes from the long-wavelength photometry (Fig. 4, Table 2), where 3mm, 2mm, $870\mu\text{m}$, and $450\mu\text{m}$ fluxes suggest a similar range of $2.5 < z < 4.5$ for a likely range of SMG dust temperatures, $25\text{ K} < T_d < 45\text{ K}$.

While these constraints may not seem very useful, the fact that we have a solid line detection at 150.6 GHz means that only three possible ^{12}CO identifications provide redshifts in this range: $^{12}\text{CO}(4-3)$ at $z = 2.82$, $^{12}\text{CO}(5-4)$ at $z = 3.58$, or $^{12}\text{CO}(6-5)$ at $z = 4.37$. Aided by these photometric redshift estimates, in two subsequent PdBI followup observations we searched for $z = 3.58$ $^{12}\text{CO}(4-3)$ at 100.4 GHz, and then at 91.5 GHz searched simultaneously for $z = 2.82$ $^{12}\text{CO}(4-3)$ and [CI] at $z = 4.37$. With a detection of a second line (Fig. 2) we confirmed the redshift

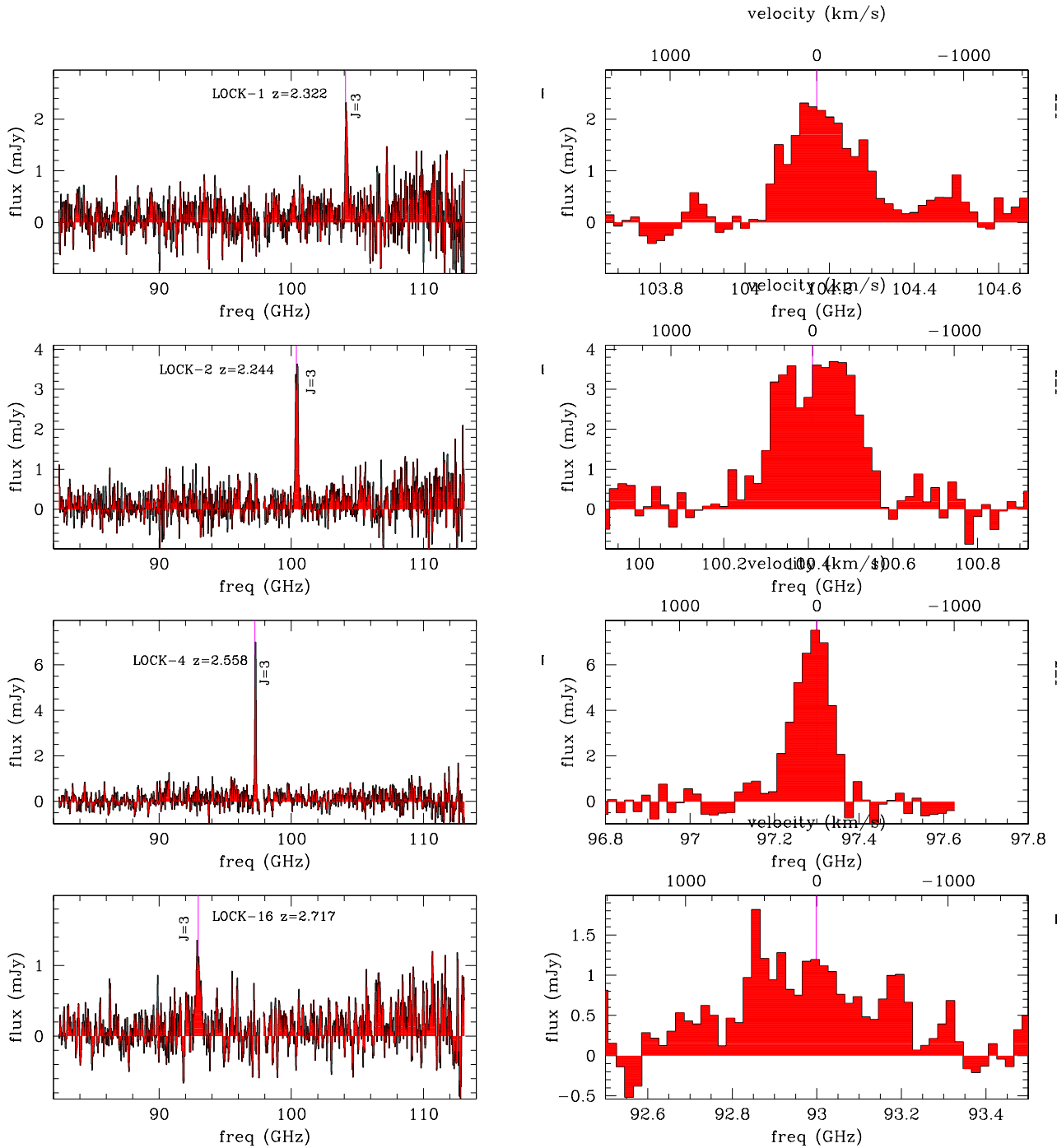


Figure 4. A composite of all spectral scans (2 tunings) towards CDF-N and Lockman sources, shown at a velocity resolution of 60 km s^{-1} . ^{12}CO and $[\text{CI}]_{2-1}$ emission lines are marked the latter corresponding to $^{12}\text{CO}(5-4)$. For the single line identifications, all other possible redshifts have been fit, and no other significant lines are found to lie near the implied frequencies of other lines.

$z=2.816$ for one of the most intrinsically luminous galaxies in the distant Universe ($L_{\text{FIR}} \sim 5 \times 10^{13} L_{\odot}$, § 3.3) and secured a second ^{12}CO line for astrophysical diagnostics. Blind ^{12}CO redshifts for unlensed SMGs are still exceedingly rare in the literature. We are only aware of Daddi et al. (2009) GN20 at $z = 4.05$ (a truly serendipitous discovery), and the $z = 5.2$ for HDF850.1 (Walter et al. 2012).

3.2 Individual source properties

CDFN-1 is very bright at $850\mu\text{m}$, but shows no sign of lensing – the nearest galaxy detected is the low-mass star forming galaxy BX951 $2.9''$ away ($z=2.3053$, $M^* = 2 \times 10^9 M_{\odot}$). It is thus not suffering from differential lensing and associated modelling issues and biases that could affect our interpretation of the ^{12}CO lines. The ^{12}CO spectra are shown zoomed in at a velocity resolution of 60 km s^{-1} in Fig. 3. Both lines are detected at high significance (11.3σ and

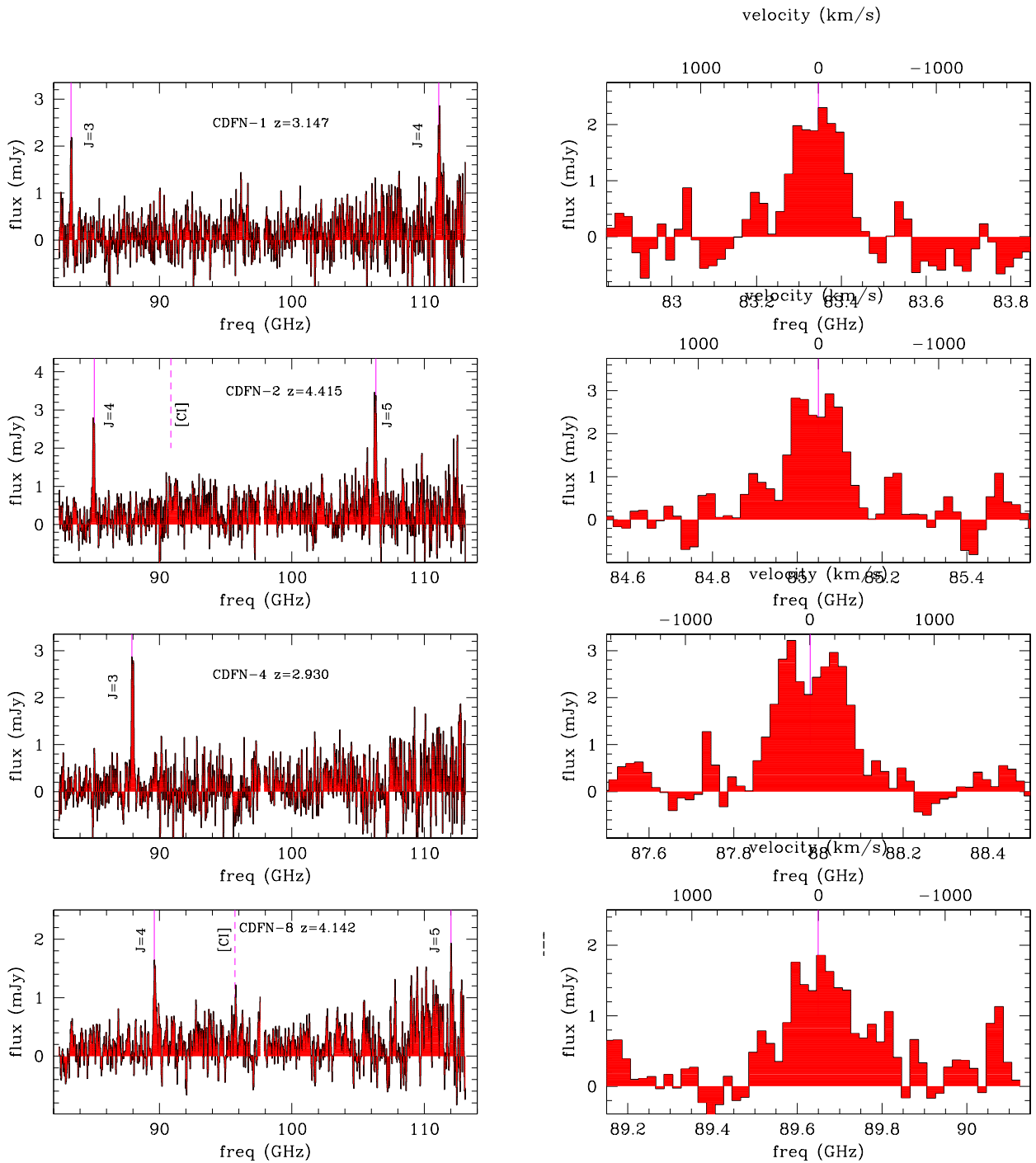


Figure 5. Zoomed in lines of lowest transition of CO detected in the spectral scans.

6.9σ for continuum subtracted (3–2) and (5–4) lines respectively, in integrated intensity). The line profiles for both lines are similar and well described by a double Gaussian with a peak separations of 585 and 530 km s^{-1} for (3–2) and (5–4) ^{12}CO lines respectively, and individual peak FWHMs of $\sim 330\text{--}470 \text{ km s}^{-1}$. While the (3–2) line shows an apparent peak flux asymmetry compared with the (5–4) peaks, in fact the flux ratios of the blue and red lines are quite similar, $r_{53,blue}=0.69\pm 0.12$ and $r_{53,red}=0.59\pm 0.09$. The parameters derived from Gaussian fits to both line profiles are given in Table 3. We find only marginal evidence for any spatial separa-

tion in the two peaks of either of the ^{12}CO lines $< 1''$. The frequencies unambiguously identify the lines as CO(3–2) and CO(4–3). Combining the centroids of both lines, we derive a variance-weighted mean redshift of $z = 3.147 \pm 0.001$. While the observed frequencies might also be interpreted as $^{12}\text{CO}(6\text{--}5)$ and $^{12}\text{CO}(10\text{--}9)$ at $z = 6.64$, the ^{12}CO ladder is not equidistant in frequency which results in small differences for the frequency separation of the line-pairs as a function of rotational quantum number. The frequency separation is 58.58 and 58.53 GHz for the ^{12}CO line-pairs at redshifts 2.82 and 6.64 respectively. Our observations yield

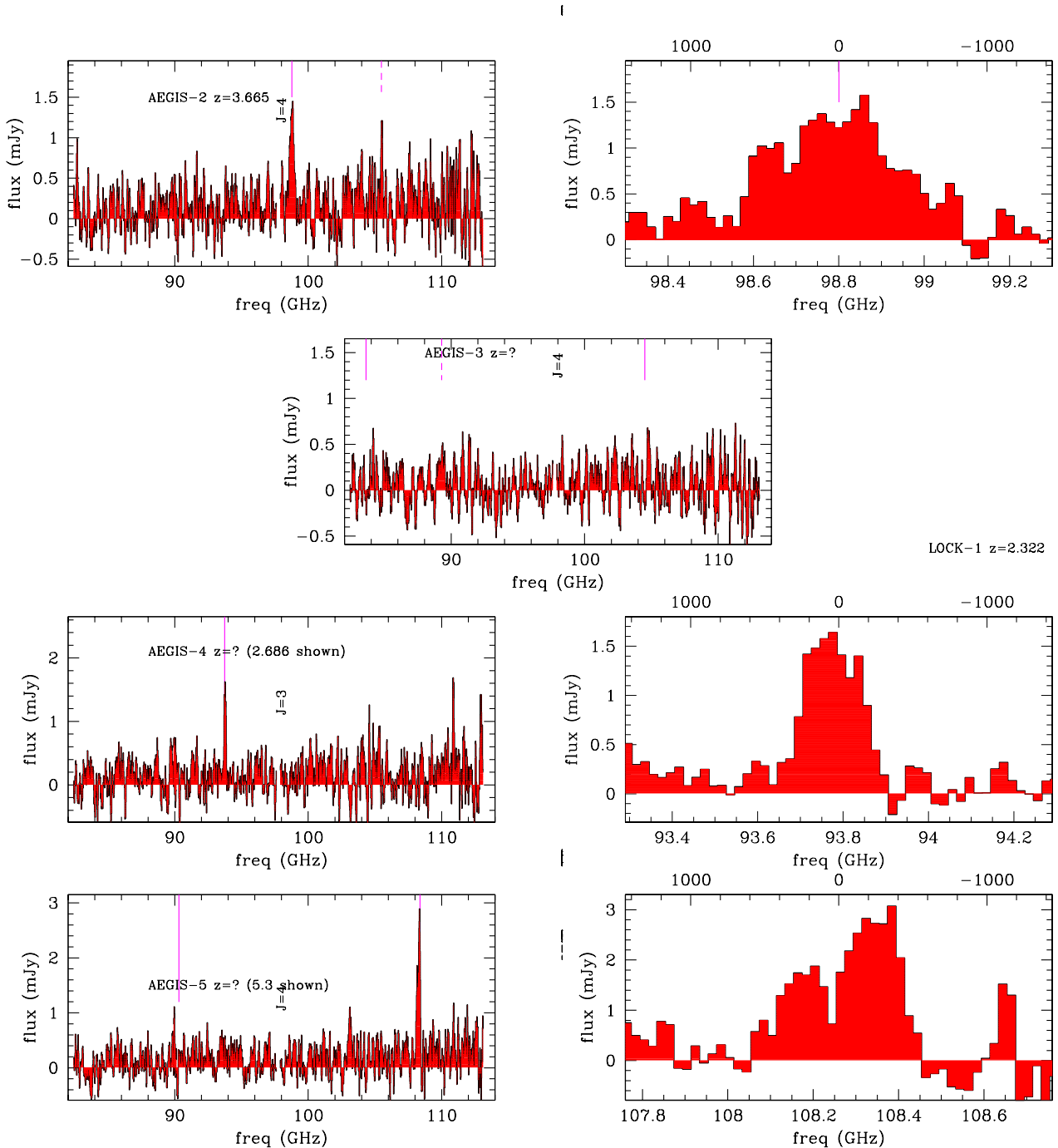


Figure 6. Zoomed in lines of lowest transition of CO detected in the spectral scans.

$\delta\nu = 58.58 \pm 0.02$ GHz, clearly consistent with the former, and supported by the photometric redshift.

With the precise redshift and the observed ^{12}CO line luminosities in hand, we can estimate the molecular gas content. Where we have two line detections, the observed global $^{12}\text{CO}(4-3)$ to $^{12}\text{CO}(3-2)$ line ratio (average 0.7 ± 0.2) implies that the CO emission is likely sub-thermally excited. The average line ratio reported by Bothwell et al. (2013) for a sub-sample of their 30 SMGs is $r_{53} = 0.62$. This line ratio is similar to that observed for SMM J16359+6612 (Weiss et al. 2005) and we use a similar scal-

ing to estimate a $^{12}\text{CO}(1-0)$ line luminosity of $L' \approx 1.86 \cdot 10^{11} \text{ K km s}^{-1} \text{ pc}^2$. The molecular gas masses have an average $M_{\text{H}_2} \approx 2.1 \cdot 10^{11} M_{\odot}$ using a standard ULIRG conversion factor of $1.0 M_{\odot} (\text{K km s}^{-1} \text{ pc}^2)^{-1}$ found for typical $z \sim 2.5$ SMGs in Bothwell et al. (2013), and including a 15% contribution from Helium. (Downes et al. 1998 adopted $0.8 M_{\odot} (\text{K km s}^{-1} \text{ pc}^2)^{-1}$).

Table 1. fluxes and redshifts.

source	RA (GHz)	Dec (hr)	Beam (mJy)	s250	s350	s500	s850	z	comment
cdfn1	12:35:55.889	+62:22:39.15	2x1.9'	30.3 3	41.0 4	47.8 6	17.0 1.5	3.147	CO32, CO43 500um peaking
cdfn2	12:35:51.467	+62:21:47.38	5x4'	19.3 3	29.7 4	34.8 6	13.7 1.5	4.415	CO43, CO54, CI 500um peaking
cdfn4	12:37:30.736	+62:12:59.77	5.5x3'	48.7 3	55.0 4	46.8 6	14.9 1.5	2.930	CO32 350um peaking
cdfn8	12:36:27.182	+62:06:05.82	2.2'	9.6 3	22.7 4	30.3 6	11.5 1.5	4.142	CO43, CO54, CI 500um peaking
lock1	10:46:45.083	+59:15:41.95	5x4'	27.2 3	36.6 4	30.0 6	12.3 1.5	2.322	CO32 (possible it's CO43 with weak CI?) 350um peaking
lock2	10:46:35.860	+59:07:48.15	6.4x5'	35.7 3	39.0 4	37.3 6	12.2 1.5	2.244	CO32 350um peaking
lock4	10:48:03.624	+58:54:21.30	6x6'	58.4 3	70.0 4	54.7 6	14.1 1.5	2.558	CO32 350um peaking
lock16	10:44:56.706	+58:49:59.78	4x5'	14.3 3	21.7 4	24.2 6	11.9 1.5	3.957	CO43 or 2.717 CO32 500um peaking
aeg2	14:15:57.527	+52:07:12.40	3x2'	19.0 3	36.0 4	38.0 6	13.8 1.5	3.665	CO43, CI 500u peaking barely
aeg3	14:15:47.066	+52:13:48.38	3'	65.4 3	53.7 4	48.6 6	16.4 1.5	1.194	CO21 2.293 CO32 ? 250um peaking
aeg4	14:19:14.246	+53:00:33.58	3'	23.3 3	25.4 4	21.3 6	11.1 1.5	2.686	CO32 ? 350um peaking
aeg5	14:19:19.983	+52:56:09.05	2.5x3'	27.1 3	35.7 4	25.6 6	14.4 1.5	2.187	CO32 ? 350um peaking ... CO43 z=3.250' weak line

^a 5-Antenna integration.^b per 50MHz channel.